

## Hosing Instability Suppression in Self-Modulated Plasma Wakefields

J. Vieira,<sup>1,3,\*</sup> W. B. Mori,<sup>2</sup> and P. Muggli<sup>3</sup>

<sup>1</sup>GoLP/Instituto de Plasmas e Fusão Nuclear, Instituto Superior Técnico, Universidade de Lisboa, 1049-001 Lisboa, Portugal

<sup>2</sup>Department of Physics and Astronomy, University of California Los Angeles, California 90095, USA

<sup>3</sup>Max-Planck-Institut für Physik, 80805 München, Germany

(Received 13 December 2013; published 21 May 2014)

We show that the hosing instability can be suppressed after the saturation of the self-modulation instability of a long particle bunch if the plasma density perturbation is linear. We derive scalings for maximum bunch tilts and seeds for the self-modulation instability to ensure stable propagation beyond saturation of self-modulation instability. Numerical solutions of the reduced hosing equations and three-dimensional particle-in-cell simulations confirm our analytical findings. Our results may also apply when a train of particle bunches or laser pulses excites a linear wake.

DOI: 10.1103/PhysRevLett.112.205001

PACS numbers: 52.40.Mj, 52.35.-g, 52.65.Rr

Plasma accelerators are witnessing impressive advances [1], with experiments using 1–100 J, focused ( $\sigma_r \approx 10 \mu\text{m}$ ) and short ( $\sigma_z \approx 10 \mu\text{m}$ ) laser wakefield accelerator [2] or particle plasma wakefield accelerator (PWFA) [3] drivers to excite large amplitude plasma wakefields for 1–40 GeV electron acceleration in 1–80 cm [4,5]. To increase energy gain beyond this limit,  $\gtrsim 10$  kJ, short ( $\sigma_z \approx 100 \mu\text{m}$ ) proton bunches have been proposed as drivers for 600 GeV electron acceleration in 600 m long plasmas [proton driven plasma wakefield accelerator (PDPWFA) [6]]. However, proton bunches available today are longer than the plasma wavelength  $\lambda_p$  even at low plasma densities ( $n_0 \approx 10^{14}$ – $10^{16} \text{ cm}^{-3}$ ). These bunches are thus suited to drive large acceleration gradients ( $\sim 1$  GeV/m) through the self-modulation instability (SMI) [7,8], provided that plasma ion motion is avoided [9]. Unlike current PWFA experiments, which excite strongly nonlinear wakes [10], PDPWFA experiments will then operate in the linear regime. SMI experiments of electron and positron bunches were also proposed to test key physics of the PDPWFA [11].

The hosing instability (HI), which can lead to bunch breakup [12,13], is considered a major impediment for the self-modulated (SM) PWFA, since SMI and HI growth rates are similar [15]. Bunch breakup could thus occur before SMI saturation. Moreover, the HI could lead to bunch breakup even after saturation of the SMI, where particle acceleration can occur. The mitigation of the HI is therefore crucial for SM PWFAs.

In this Letter we show that hosing can be stabilized if the SMI can reach a fully saturated state and the plasma density perturbations ( $\delta n_p/n_0 \ll 1$ ) are much smaller than the background plasma density; i.e., the wakefields are in the linear regime. We determine the amount of seeding for SMI saturation before beam breakup due to the HI. If this occurs, stable wakefields in the SM-PWFA regime can be excited and maintained over long acceleration

distances. Beam breakup due to the HI can still occur when beam density perturbations reach 100% in the blowout regime and in this case stabilization might be achieved through the use of a correlated energy spread. Numerical solutions of the reduced set of differential equations for the bunch centroid evolution and three-dimensional (3D) particle-in-cell (PIC) simulations with OSIRIS [14] confirm analytical findings.

We start by describing centroid displacements  $x_c$  of bunches with density profiles given by  $n_b = (n_{b0} r_{b0}^2/r_b^2)[\Theta(r_b - r) + \delta(r - r_b)x_c \cos \theta]$ , where  $n_{b0}$  is the initial bunch density,  $\Theta(x)$  is the Heaviside function, and where  $\delta(x)$  is the Dirac delta function. The bunch radius is  $r_b$ , the transverse coordinates are  $(x, y)$ ,  $r_{b0} = r_b(z = 0, \xi)$ ,  $r = \sqrt{x^2 + y^2}$ , and the azimuthal angle is  $\theta$ . In the narrow bunch limit ( $k_p r_b \ll 1$ ), hosing can be described by [15]

$$\frac{\partial^2 x_c}{\partial z^2} = k_\beta^2 \int_{-\infty}^{\xi} n_{||}(\xi') k_p [x_c(\xi') - x_c(\xi)] \sin[k_p(\xi - \xi')] d\xi', \quad (1)$$

where  $k_\beta^2 = k_p^2 m_e n_{b0} / (2\gamma m_b n_0)$  and  $k_p = \sqrt{4\pi n_0 e^2 / m_e}$  are the betatron and plasma wave numbers,  $e$  and  $m_e$  are the electron charge and mass, and  $q_b$ ,  $m_b$ ,  $\gamma = 1/\sqrt{1 - v_b^2/c^2}$  are the bunch particles' charge, mass, and relativistic factor, and  $v_b$  is its velocity. The co-moving frame coordinate,  $\xi = z - v_b t$  is used, where  $\xi$  is the location within the beam, and  $n_{||} = r_{b0}^2/r_b^2$ .

Similarly to laser hosing [16] Eq. (1) can be recast as

$$\left( \frac{\partial^2}{\partial z^2} + \frac{ek_\beta^2 \delta n_p}{q n_0} \right) x_c = k_\beta^2 x_w, \quad (2a)$$

$$\left( \frac{\partial^2}{\partial \xi^2} + k_p^2 \right) x_w = k_p^2 n_{||} x_c, \quad (2b)$$

$$\left(\frac{\partial^2}{\partial \xi^2} + k_p^2\right) \frac{\delta n_p}{n_0} = \frac{q_b k_p^2}{e} n_{\parallel}, \quad (2c)$$

where we identify  $x_w$  as the wake centroid. Equations (2a)–(2c) show that hosing occurs due to the coupling of  $x_c$ , oscillating in  $z$  at  $k_p(\delta n_p/n_0)^{1/2}$ , and  $x_w$ , oscillating in  $\xi$  at  $k_p$ . The coupling term also includes the beam density  $n_{\parallel}$ , which drives the harmonic oscillator Eq. (2c) for  $\delta n_p/n_0$ . When linearized, i.e., when the beam density and the wake amplitudes are fixed, these equations provide various regimes of growth for hosing that can be identified by which of the first two equations in Eqs. (2) is nearly resonant. When  $x_w$  oscillates near  $k_p$ , the instability is in the long pulse regime, which is the regime of interest for current long beam research where the number of exponentiations scales as  $\Gamma z \propto (n_{\parallel} k_p^2 z^2 k_p \xi)^{1/3}$ .

If one wants to couple the SMI with the HI an additional equation that relates the evolution of the beam density to the wake amplitude is needed [15]. However, coupling of a self-modulated beam or a train of beamlets with the HI can be studied without this additional equation. Analysis of Eqs. (2) indicates that a train of bunches can propagate without significant centroid oscillations for  $k_p z \gg 1$ . This is demonstrated in Fig. 1(a), comparing numerical solutions to Eq. (1) or Eq. (2) for an electron bunch with a flattop density profile ( $n_{\parallel} = 1 = cst$ ) with a sharp rise (black) and for a train of bunches (red) after  $k_p z = 15$ . The bunch train profile is shown in Fig. 1(b) (red) and it was taken from a 3D PIC simulation (described later) after a long beam had undergone the SMI. For the bunch train [Fig. 1(a)]  $x_c$  is up

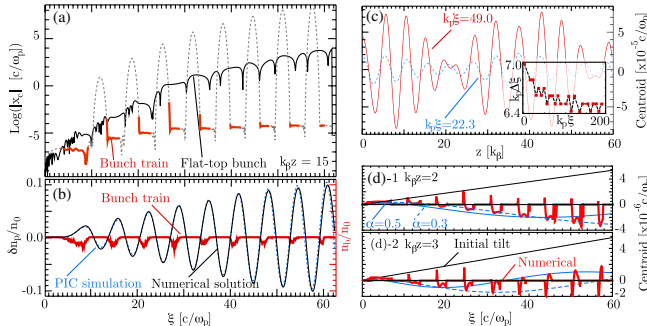


FIG. 1 (color online). (a) Numerical solutions for the centroid evolution for a flattop bunch (black-solid thinner line) and at the locations of a train of bunches (red-solid thicker line). The dashed gray line shows the centroid solution for the train of bunches at any  $\xi$ . (b) Corresponding bunch density profile (red-solid thicker line), plasma density perturbations retrieved from a 3D PIC simulation (blue-dashed line) and corresponding numerical solution (black-thinner solid line) using Eq. (2c). (c) Numerical solution for  $x_c$  for a train of Dirac-delta-like bunches [with length  $k_p \sigma_z = 0.1$  and density  $n_l = n_0/(k_p \sigma_z)$ ] located at maximum focusing field regions. The inset shows the relative distance between beamlets. (d) Panels 1 and 2. Numerical (red-thicker solid line) and analytical (blue-solid and dashed lines) solutions for the centroid evolution of a collection of beamlets. The initial centroid displacement is  $x_{c0} = 8.93 \times 10^{-8} \xi$ .

to 6–7 orders of magnitude smaller than for the  $n_{\parallel} = 1$  case, demonstrating possible suppression of hosing for fully self-modulated beams.

Hosing of a fully self-modulated beam or a train of bunches cannot be described in terms of the often quoted asymptotic solutions and regimes such as the long pulse regime. As the SMI occurs and  $n_{\parallel}$  becomes modulated the coupling term on the right-hand side of Eq. (2b) leads to harmonic generation of each quantity. As the number of harmonics increases the analysis of the interaction between the HI and the SMI becomes more difficult to analyze. Therefore, to understand hosing suppression in the wake driven by a train of bunches we consider a particle model with  $n_{\parallel} \equiv n_{\parallel}^{\text{SM}} = \sum_{l=0}^m k_p^{-1} n_l \delta(\xi - \xi_l)$ , where  $\xi_l$  is the location in  $\xi$  of the  $l$ th beamlet (or particle), and where  $k_p^{-1} n_l$  is proportional to its charge. Similar models were employed to investigate beam breakup in rf accelerators [17] and to study trapped particle instabilities in plasma waves [18]. Inserting  $n_{\parallel}^{\text{SM}}$  into Eq. (2) yields

$$\frac{\partial^2 x_m}{\partial z^2} + x_m(z) k_p^2 \left(\frac{\delta n_p}{n_0} \frac{q}{e}\right)_m = k_p^2 \sum_{l=0}^m n_l w_l x_l(z), \quad (3)$$

where  $x_m = x_c(z, \xi_m)$ ,  $(\delta n_p/n_0)_m = \sum_{l=0}^m n_l \sin[k_p(\xi_l - \xi_m)]$  is the amplitude of plasma density fluctuations at  $\xi = \xi_m$ , and  $w_l = \sin[k_p(\xi_l - \xi_m)]$  is a weighting factor. Equation (3) shows that  $x_m$  is described by a driven harmonic oscillator with natural frequency  $k_m^2 = k_p^2((q/e)\delta n/n_0)_m$ . The driving term is the weighted centroid oscillations of the preceding beamlets,  $\sum_l n_l w_l x_l$ .

To understand how hosing of a train of short bunches evolves, we examine the first few terms in Eq. (3) with  $n_l = 1$ , i.e., implicitly assuming that the wake perturbation is enough to guide the beam with given emittance. For  $m = 0$ ,  $\partial^2 x_0/\partial z^2 = 0$ . If  $\partial x_0/\partial z = 0$  at  $z = 0$ , then  $x_0 = x_{c0}$ . For  $m = 1$ ,  $\partial^2 x_1/\partial z^2 + k_p^2(q/e) \sin[k_p(\xi_0 - \xi_1)](x_1 - x_0) = 0$ . For  $x_0 = 0$  and  $\partial x_1/\partial z = 0$  then  $x_1 = x_{1c} \cos[z k_p \sqrt{(q/e) \sin[k_p(\xi_0 - \xi_1)]}]$ . Bounded  $x_1$  centroid oscillations occur when the beamlet  $m = 1$  resides in focusing regions ( $(q/e) \sin[k_p(\xi_0 - \xi_1)] > 0$ ), for which  $x_1$  oscillates at  $k_1 = k_p \sqrt{(q/e) \sin[k_p(\xi_0 - \xi_1)]}$ . For  $m = 2$ ,  $\partial^2 x_2/\partial z^2 + k_p^2 x_2(q/e)(\sin[k_p(\xi_0 - \xi_2)] + \sin[k_p(\xi_1 - \xi_2)]) = w_1 k_p^2 x_{1c} \cos[z k_p \sqrt{(q/e) \sin[k_p(\xi_0 - \xi_1)]}]$  where  $w_1 = \sin[k_p(\xi_1 - \xi_2)]$ . Bounded oscillations also require that  $x_2$  resides in focusing regions with  $(q/e)(\sin[k_p(\xi_0 - \xi_2)] + \sin[k_p(\xi_1 - \xi_2)]) > 0$ . In this case, the equation of motion for  $x_3$  is a driven harmonic oscillator. The driving term oscillates at  $k_1 = k_p \sqrt{(q/e) \sin[k_p(\xi_0 - \xi_1)]}$ , and the natural frequency is  $k_2^2 = k_p^2(q/e)(\sin[k_p(\xi_0 - \xi_2)] + \sin[k_p(\xi_1 - \xi_2)])$ . Hence, ensuring  $k_2 \neq k_1$  avoids resonant  $x_2$  oscillations and rapid growth. By extending this argument to the following beamlets it can be recognized that avoiding resonant centroid growth requires that every beamlet oscillates at a different frequency. This is satisfied for fully

self-modulated bunches in the linear regime, where each beamlet resides in focusing regions and the amplitude of the focusing field (and wave number) increases for each beamlet. The natural frequency can also vary if the spacing between bunches varies or if there is an energy chirp on the beam ( $k_\beta \propto 1/\sqrt{\gamma}$ ).

To illustrate hosing suppression, we present in Fig. 1(c) numerical solutions for a case where short beamlets are in regions of maximum focusing fields, as in a self-modulated scenario. We use Eqs. (2) for very short bunches, which is then equivalent to Eq. (3). Figure 1(c) demonstrates that  $(x_c - x_{c0})/x_{c0} \ll 1$  for  $k_\beta z \gg 1$ , in agreement with the results for the more realistic bunch train of Figs. 1(a)–1(b). Figure 1(b) superimposes the position of each beamlet in the wake it excites, showing that the bunch train considered in Fig. 1(a) is in focusing regions.

Numerical solutions of Eq. (2) show that finding separations  $\Delta\xi_m$  between beamlets that ensure they reside in maximum focusing fields is challenging as  $\Delta\xi_m$  depends on their relative position within the bunch train, and on their length and density profile. Therefore, producing a train of bunches in the conditions for HI suppression while making a wake over large distances would be very challenging experimentally. For example, the inset of Fig. 1(c) shows how the optimal spacing varies for beamlets for one case. Long bunches self-consistently evolve into this optimal configuration through the SMI. This can be seen in Fig. 1(b), which also shows that in this case linear wakes are still excited during the nonlinear stage of the SMI. To demonstrate this, we show in Fig. 1(b) that the numerical solution to Eq. (2c) using the simulation  $n_{||}$  and the corresponding  $\delta n_p/n_0$  retrieved from the simulation are indistinguishable.

It is possible to obtain analytical expressions for  $x_m$  in self-modulated regimes if we simplify Eq. (3) by assuming constant  $w_l = \alpha$  and  $k_m^2 = \alpha k_\beta^2 \sum_l n_l$ . This approximation corresponds to wakefields growing secularly along the bunch and to each beamlet equally driving the oscillations of following beamlets. Note that the actual value of  $\alpha$  depends on the exact density profile of each beamlet, for which no analytical predictions are available. Under the above assumptions we can replace the sums by integrals whereby Eq. (3) becomes

$$\left(\frac{\partial^2}{\partial z^2} + \alpha k_\beta^2 \int_{-\infty}^{\bar{\xi}} k_p n_{||}(\xi') d\xi'\right) x_c = \alpha k_\beta^2 \int_{-\infty}^{\bar{\xi}} k_p x_c(\xi') n_{||}(\xi') d\xi', \quad (4)$$

where  $\bar{\xi} = \xi\sigma_z/\Delta\xi$  is a new variable that runs only through regions where  $n_{||} \neq 0$ . We can solve Eq. (4) assuming  $n_{||} = 1$  (i.e., the charge on each beamlet is constant) by differentiating Eq. (4) once in  $\bar{\xi}$  and by solving the resulting equation for  $\partial x_c/\partial \bar{\xi}$  using  $x_{c0} = \delta_{\text{HI}} \bar{\xi}$  and  $\partial x_{c0}/\partial z = 0$  yielding

$$k_p x_c = \frac{2\delta_{\text{HI}}}{\alpha k_\beta^2 z^2} [-1 + \cos(N_{\text{flat}}) + N_{\text{flat}} \sin(N_{\text{flat}})], \quad (5)$$

where  $N_{\text{flat}} = k_\beta z \sqrt{\alpha k_p \bar{\xi}}$ . Equation (5) indicates that  $k_p x_c \propto \delta_{\text{HI}} \sqrt{\alpha k_p \bar{\xi}}/(k_\beta z)$  demonstrating HI damping after SMI saturation for  $k_\beta z \gg 1$ . In panels 1 and 2 of Fig. 1(d) we compare numerical solutions of Eq. (2) using  $n_{||}$  from Fig. 1(b) with Eq. (5) for  $w_l = 0.3$  or  $w_l = 0.5$  and with constant  $n_{||}$  which is the average of the actual distribution. Figure 1(d) shows that the numerical solution for  $x_c$  varies within each beamlet because the betatron frequency is  $\xi$  dependent within each bunch. The derivation of Eq. (5) assumes that the betatron frequency is constant (i.e., at a value of  $k_\beta \alpha^{1/2}$ ) and hence does not take this effect into account. Nevertheless, there is agreement with the peaks of the numerical solution for  $x_c$  and the analytical solution for  $k_\beta z \lesssim 3$ . For  $k_\beta z \gtrsim 4$  the agreement is worse because the assumption of a constant  $\alpha$  becomes progressively worse. We also note that the values for the weights  $w_l$  vary between 0.8 and 0.2 from the front to the back of the bunch train.

Our analysis shows that hosing suppression occurs in the linear regime because the betatron frequency of each bunch varies along the train. In the nonlinear regime driven by negatively charged bunches, the focusing fields are set by the ion column density. Thus, all beamlets oscillate at the same frequency, and hosing can still grow. Simulations demonstrate that electron bunches with a correlated energy spread could nevertheless be used to damp or suppress hosing in this case because  $k_\beta \propto 1/\sqrt{\gamma}$  now varies along the bunch. In addition, when the beamlets are not short when compared with  $\lambda_p$ , as is often the case, the variation of the accelerating field across each bunch could also contribute to damp the HI. For positively charged bunches, most of the bunch defocuses during the growth of the SMI in the blowout regime. Thus, stable propagation for positively charged drivers requires wakefields in the linear regime. The HI suppression mechanisms mentioned above are similar to Balakin-Novokharsky-Smirnov (BNS) damping in rf linear accelerators [19].

We can estimate the bunch density after SMI saturation considering  $n_{b0} r_{b0}^2 = n_{b(\text{sat})} r_{b(\text{sat})}^2$ , where  $n_{b(\text{sat})}$  and  $r_{b(\text{sat})}$  refer to the matched bunch density and radius after SMI saturation [20]. By assuming that the wake grows secularly along the self-modulated bunch,  $n_{b(\text{sat})} \approx n_{b0} r_{b0}^2 [(\gamma k_p^2 / 2\epsilon_N^2) (n_{b0}/n_0) (m_e/m_b) (\sigma_z/\lambda_p)]^{1/2}$ , where  $\epsilon_N$  is the normalized emittance. For a PDPWFA with  $n_{b0}/n_0 \approx 10^{-2}$ ,  $\sigma_z \approx 10$  cm,  $n_0 \approx 10^{14}$  cm $^{-3}$ ,  $r_{b0} \approx 200$   $\mu$ m, and  $\epsilon_N \approx 3$  mm mrad,  $n_{b(\text{sat})}/n_0 = 0.04$ . Furthermore, PDPWFA simulations show that emittance can increase by an order of magnitude, such that  $n_{b(\text{sat})}/n_0$  becomes even lower. Thus, the wakefield will still be in the linear regime in experiments, and hosing can be stabilized after SMI saturation.

Stable wake excitation in a SM PWFA requires SMI saturation before bunch breakup due to the HI. This

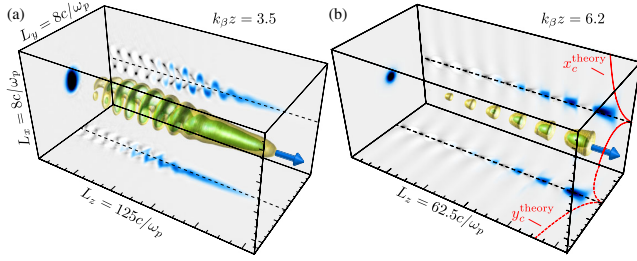


FIG. 2 (color online). OSIRIS simulation results: Bunch density isosurfaces (color-yellow and green; black and white-lighter and darker gray). Projections show electron bunch (color-blue, black and white-darker gray) and plasma density (lighter gray). (a) Bunch with smooth temporal profile. (b) Bunch with sharp-rise long-fall current profile for SMI seeding. The dashed lines show HI theoretical predictions for non-self-modulated bunches.

condition can be fulfilled when the SMI seed is larger than for HI; i.e., the initial focusing force that seeds hosing ( $\langle W_{\perp, \text{HI}} \rangle$ ) needs to be smaller than that seeding self-modulation ( $\langle W_{\perp, \text{SMI}} \rangle$ ). This is the same as having the seed for  $x_w$  being smaller than the seed for  $\delta n_p / n_0$ . Among several SMI seeding mechanisms [21–23] we consider seeding by bunches with short rise times [24] for which  $\langle W_{\perp, \text{SMI}} \rangle \propto k_p^2 k_p r_{b0}$ . Beam tilts that seed hosing lead to  $\langle W_{\perp, \text{HI}} \rangle = k_p^2 k_p \sigma_z \delta_{\text{HI}}$ . Hence  $\langle W_{\perp, \text{SMI}} \rangle / \langle W_{\perp, \text{HI}} \rangle \gtrsim 1$  holds as long as  $\delta_{\text{HI}} \lesssim r_b / \sigma_z$  ( $x_{c0} = \delta_{\text{HI}} \xi$ ), consistent with Ref. [23]. Stable propagation then occurs for all beamlets whose centroid initially resides within the bunch radius, at the bunch front.

A set of 3D PIC simulations was performed with the numerical code OSIRIS [14]. See the Supplemental Material [25] for the simulation parameters. Figure 2(a) illustrates the transition between the linear stage of hosing to a nonlinear coupling between the SMI and the HI. In this case, even with a very small seed for the HI ( $k_p \delta_{\text{HI}} = 0.001$ ) and essentially no SMI seeding, the HI strongly breaks up the bunch density after a short propagation distance ( $k_{\beta} z = 3.5$ ) and before the SMI can grow. Figure 2(b) shows results from the half bunch. Even with an initial HI seed 10 times larger than in the case of Fig. 2(a) ( $k_p \delta_{\text{HI}} = 0.01$ ), the bunch is free of the HI. The beam becomes fully self-modulated and then stably propagates over a longer distance into the plasma ( $k_{\beta} z = 6.2$ ). In this case, existing hosing theory for flat bunches significantly overestimates  $|x_c|$  [26].

Figures 3(a)–3(b) show that hosing suppression also occurs for flattop bunches with different initial tilts and with  $n_b / n_0 = 0.01$  so long as the wake is still in the linear regime after saturation. Figure 3(a) shows results from a simulation in which the tilt was small enough so that centroid variation across the entire beam was less than the initial spot size, i.e., where  $x_{c0} = \delta_{\text{HI}} \sigma_z = 0.6 r_b < r_b$ . In this case all the self-modulated beamlets propagate stably. The  $y$  direction focusing force ( $W_y = E_y - B_z$ ) increases along the bunch, resulting in betatron frequency detuning among self-modulated beamlets, which leads to HI

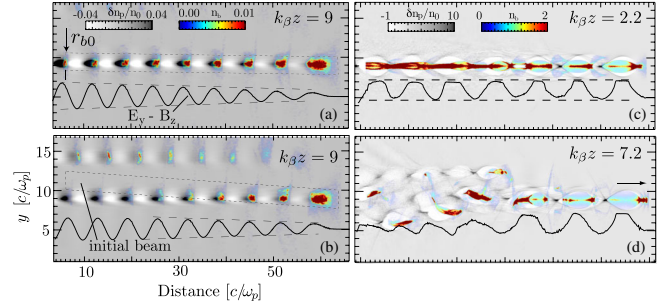


FIG. 3 (color online). OSIRIS simulation results of the propagation of the long electron bunch (color-blue red, black and white-darker gray) in a plasma (lighter gray) in the linear [(a) and (b)] and nonlinear [(c) and (d)] wakefield regime. The shape of the initial bunch profile is shown by the short dashed lines. The initial bunch radius  $r_{b0}$  is also indicated. Plasma focusing force  $E_y - B_z$  (solid lines) and envelope of  $E_y - B_z$  (long dashed lines) are also illustrated.

suppression and which is consistent with Eqs. (3) and (4). The simulation results from Fig. 1(b) correspond to on-axis lineouts from Fig. 3(a). In Fig. 3(b), results for a beam with a larger tilt are shown. In this case  $x_{c0} = \delta_{\text{HI}} \sigma_z = 3 r_b > r_b$  and only beamlets satisfying  $\xi \lesssim r_b / \delta_{\text{HI}}$  ( $x_{c0} < r_b$ ) propagate stably (i.e., those with  $k_p \xi \gtrsim 30$ ), in agreement with analytical scalings. Also in agreement with theory, additional simulations (not shown) also confirm these conclusions for positron bunches.

Figures 3(c)–3(d) illustrate the breakup of the same bunches as used in Figs. 3(a)–3(b), but with  $n_b / n_0 = 0.5$  such that the wakefields driven by the SMI eventually reach the nonlinear blowout regime. As the bunch self-modulates, the amplitude of the plasma focusing force becomes constant throughout the entire bunch train and the amplitude is the same for each bunch [solid and dashed lines in Fig. 3(c)]. As discussed earlier this prevents the suppression of the HI and the beam is seen to eventually break apart due to resonant HI growth [Fig. 3(d)]. Other wakefield saturation mechanisms (e.g., due to fine scale mixing of electron trajectories [27]) could also lead to HI growth.

In conclusion, we have shown that the hosing instability of long particle beams can be suppressed and stabilized if the beam first becomes fully self-modulated and the resulting wake and density perturbations remain in the linear regime. This requires that the seed for the SMI is larger than for the HI. Fully self-consistent PIC simulations show that for long particle beams with sharp rise times the beam can propagate for long distances exciting a wakefield that could be used to accelerate externally injected particles. This suppression mechanism is analogous to Balakin-Novokharsky-Smirnov damping in conventional linear accelerators. These results should also apply to a train of laser pulses [28] and this will be addressed in future work.

This work was supported by FCT (Portugal), Grant No. EXPL/FIS-PLA/0834/1012, by the European Research Council (ERC-2010-AdG Grant No. 267841), and by DOE

Grants No. DE-SC0008491, No. DE-SC0008316, and No. DE-FG02-92-ER40727, and Grant No. NSF-ACI-1339893. J. V. acknowledges the support of the Alexander von Humboldt Foundation for a postdoctoral fellowship at the Max Planck Institute for Physics in Munich. We acknowledge PRACE for access to resources on JüQueen (Jülich) and SuperMUC (Leibniz Research Center) and INCITE for use of the Titan supercomputer. We also acknowledge useful discussions with Professor Luis O. Silva and Professor Ricardo A. Fonseca.

\*jorge.vieira@ist.utl.pt

- [1] N. Patel, *Nature (London)* **449**, 133 (2007).
- [2] T. Tajima and J. M. Dawson, *Phys. Rev. Lett.* **43**, 267 (1979).
- [3] P. Chen, J. M. Dawson, R. W. Huff, and T. Katsouleas, *Phys. Rev. Lett.* **54**, 693 (1985).
- [4] X. Wang *et al.*, *Nat. Commun.* **4**, 1988 (2013); W. P. Leemans, B. Nagler, A. J. Gonsalves, Cs. Tóth, K. Nakamura, C. G. R. Geddes, E. Esarey, C. B. Schroeder, and S. M. Hooker, *Nat. Phys.* **2**, 696 (2006); S. Kneip *et al.*, *Phys. Rev. Lett.* **103**, 035002 (2009); C. E. Clayton *et al.*, *Phys. Rev. Lett.* **105**, 105003 (2010).
- [5] I. Blumenfeld *et al.*, *Nature (London)* **445**, 741 (2007).
- [6] A. Caldwell, K. Lotov, A. Pukhov, and F. Simon, *Nat. Phys.* **5**, 363 (2009); K. V. Lotov, *Phys. Rev. ST Accel. Beams* **13**, 041301 (2010).
- [7] N. Kumar, A. Pukhov, and K. Lotov, *Phys. Rev. Lett.* **104**, 255003 (2010).
- [8] C. B. Schroeder, C. Benedetti, E. Esarey, F. J. Gruner, and W. P. Leemans, *Phys. Rev. Lett.* **107**, 145002 (2011); A. Pukhov, N. Kumar, T. Tüchtmantel, A. Upadhyay, K. Lotov, P. Muggli, V. Khudik, C. Siemon, and G. Shvets, *Phys. Rev. Lett.* **107**, 145003 (2011).
- [9] J. Vieira, R. A. Fonseca, W. B. Mori, and L. O. Silva, *Phys. Rev. Lett.* **109**, 145005 (2012).
- [10] A. Pukhov and J. Meyer-ter-Vehn, *Appl. Phys. B* **74**, 355 (2002); W. Lu, C. Huang, M. Zhou, W. B. Mori, and T. Katsouleas, *Phys. Rev. Lett.* **96**, 165002 (2006).
- [11] J. Vieira, Y. Fang, W. B. Mori, L. O. Silva, and P. Muggli, *Phys. Plasmas* **19**, 063105 (2012).
- [12] E. Lee, *Phys. Fluids* **21**, 1327 (1978).
- [13] D. H. Whittum, W. M. Sharp, S. S. Yu, M. Lampe, and G. Joyce, *Phys. Rev. Lett.* **67**, 991 (1991); M. Lampe, G. Joyce, S. P. Slinker, and D. H. Whittum, *Phys. Fluids B* **5**, 1888 (1993); C. K. Huang *et al.* *Phys. Rev. Lett.* **99**, 255001 (2007).
- [14] R. A. Fonseca *et al.*, *Lect. Notes Comp. Sci.* vol. 2331/2002, (Springer Berlin, (2002).
- [15] C. B. Schroeder, C. Benedetti, E. Esarey, F. J. Gruner, and W. P. Leemans, *Phys. Rev. E* **86**, 026402 (2012).
- [16] B. J. Duda and W. B. Mori, *Phys. Rev. E* **61**, 1925 (2000).
- [17] P. B. Wilson and J. E. Griffin in *Physics of High Energy Particle Accelerators*, edited by R. A. Carrigan, F. R. Huson, and M. Month, AIP Conf. Proc. No. 87 (AIP, New York, 1982), Sec. 11.1; A. Chao in *Coherent Instabilities of a Relativistic Bunched Beam*, edited by M. Month, AIP Conf. Proc. No. 105 (AIP, New York, 1983), Sec. 2.3.
- [18] W. L. Kruer, J. M. Dawson, and R. N. Sudan, *Phys. Rev. Lett.* **23**, 838 (1969).
- [19] V. E. Balakin, A. V. Novokhatsky, and V. P. Smirnov, *Vleep: Transverse Beam Dynamics*, edited by F. T. Cole and R. Donaldson, Proceedings of 12th International Conference on High Energy Accelerators (Fermi National Accelerator Laboratory, Batavia, Illinois, 1983).
- [20] We thank the anonymous referee for this suggestion.
- [21] J. Vieira *et al.* (to be published).
- [22] W. B. Mori and T. Katsouleas, *Phys. Rev. Lett.* **69**, 3495 (1992).
- [23] C. B. Schroeder, C. Benedetti, E. Esarey, F. J. Gruner, and W. P. Leemans, *Phys. Plasmas* **20**, 056704 (2013).
- [24] Y. Fang, V. E. Yakimenko, M. Babzien, M. Fedurin, K. P. Kusche, R. Malone, J. Vieira, W. B. Mori, and P. Muggli, *Phys. Rev. Lett.* **112**, 045001 (2014).
- [25] See Supplemental Material at <http://link.aps.org/supplemental/10.1103/PhysRevLett.112.205001> for description of numerical and physical parameters for the simulations of Figures 2 and 3.
- [26] We note that the beam charge in the modulated bunch in Fig. 2(b) is 4 times smaller than in Fig. 2(a). This lower charge is because the bunch is cut on the middle, and half the charge is defocused by the SMI. The propagation distance in Fig. 2(b), however, is twice as large as for Fig. 2(a). The theoretical number of  $e$ -foldings in Fig. 2(a) should then be similar to that of Fig. 2(b), since the number of  $e$ -foldings scales as  $(n_b k_p \xi k_\beta^2 z^2)^{1/3}$ . However, centroid oscillations are much larger in Fig. 2(a) than in Fig. 2(b). In addition, simulations show that whereas the half cut bunch continues to propagate stably in Fig. 2(b), beam breakup occurs in the case of Fig. 2(a). Together with the fact that the initial tilt that seeds the hosing in Fig. 2(b) is 10 times larger than that in Fig. 2(a), Fig. 2 shows that hosing suppression can occur in the linear regime after SMI saturation.
- [27] J. M. Dawson, *Phys. Rev.* **113**, 383 (1959).
- [28] S. M. Hooker, R. Barolini, S. P. D. Mangles, A. Tünnemann, L. Corner, J. Limpert, A. Seryi, and R. Walczak, [arXiv:1401.7874](https://arxiv.org/abs/1401.7874).